

# Two Gas-Puff Staged Pinch Dynamics with Finite- $\beta$ Effects

Dr. Arshad M. Mirza,  
Physics Department,  
Quaid-i-Azam University,  
Islamabad

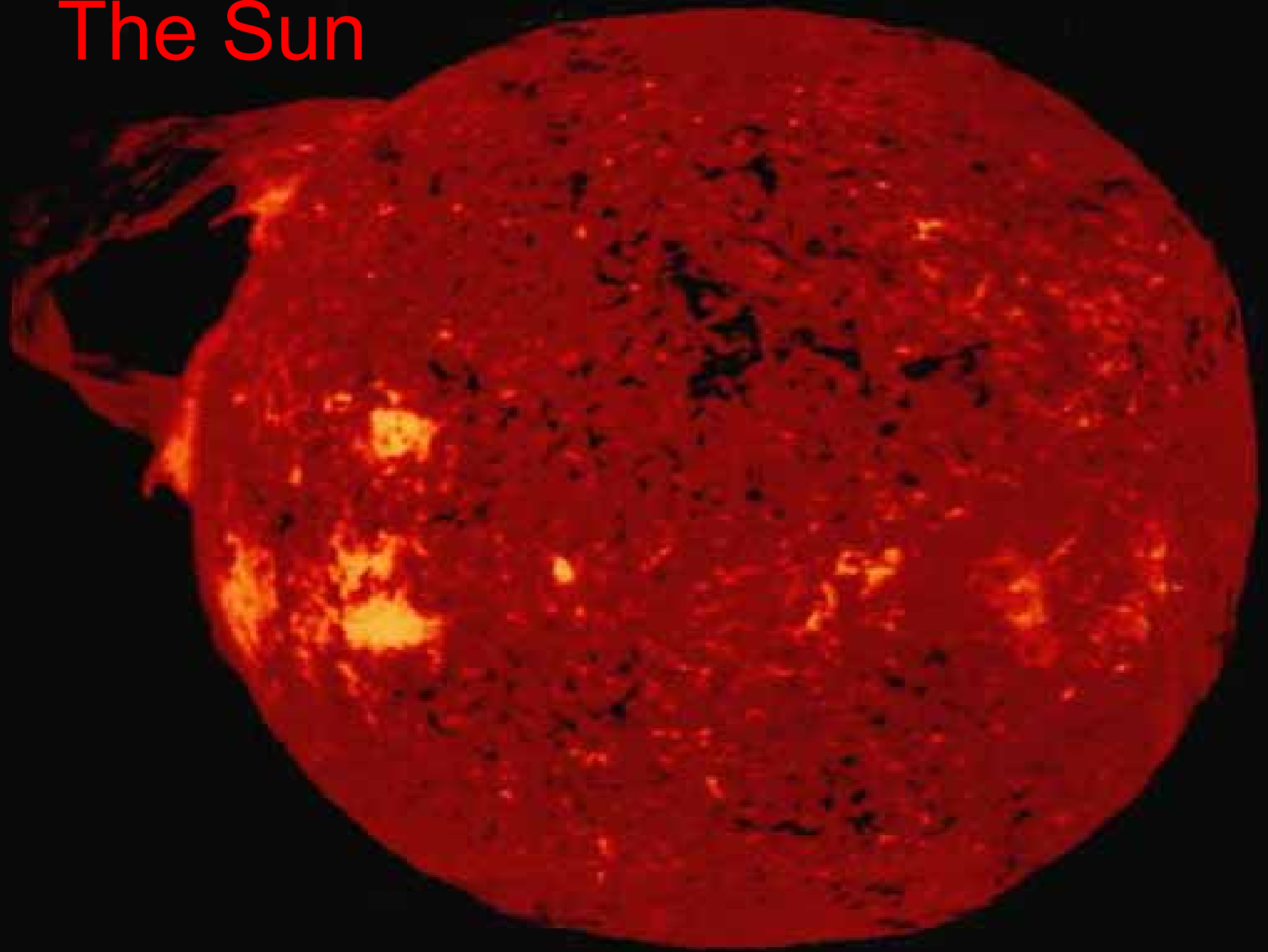
# Introduction



“Every time you look up at the sky, every one of those points of light is a reminder that *fusion power is extractable from hydrogen* and other light elements”

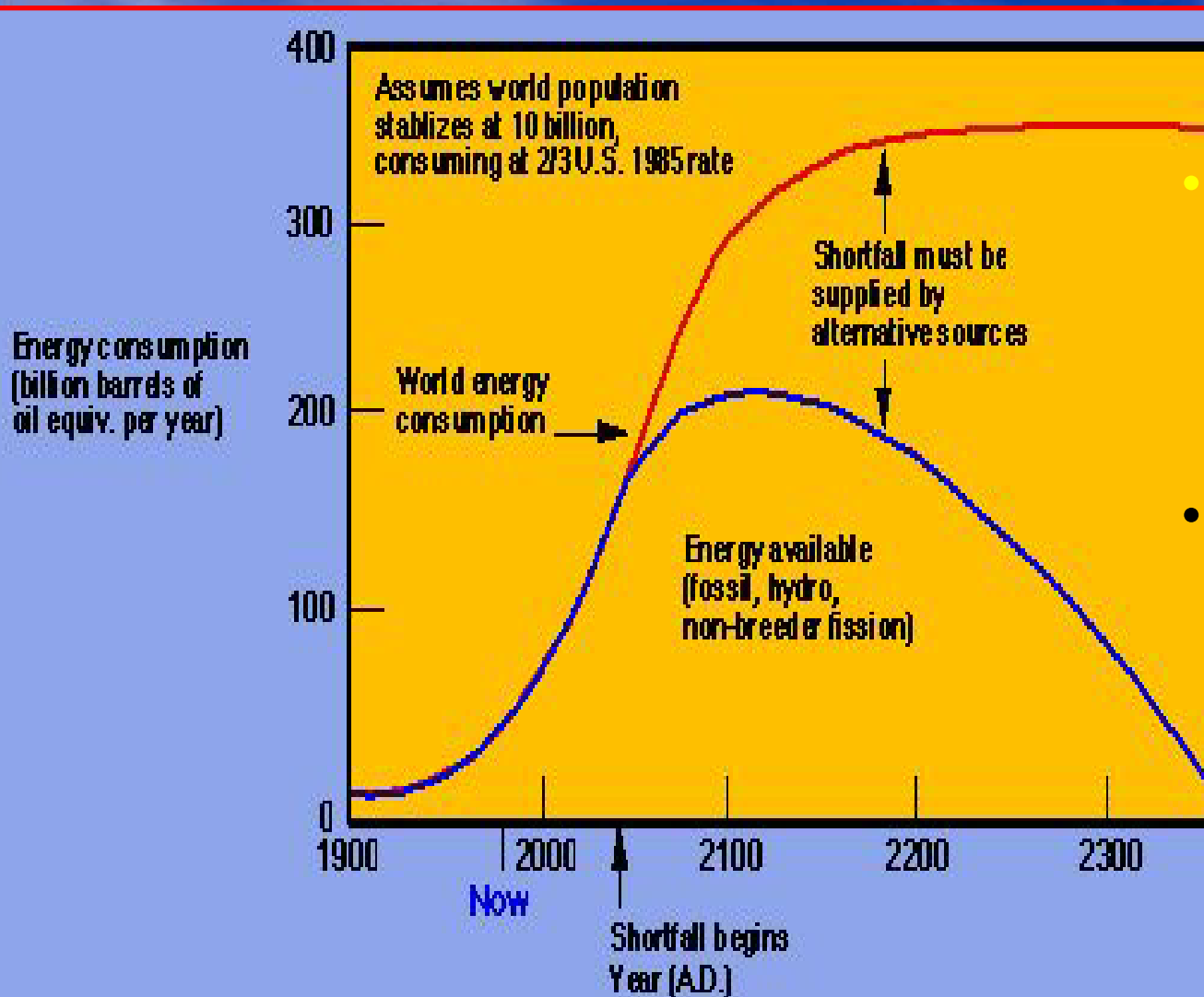
-Carl Sagan, 1991

# The Sun



# No More Fossil Fuel?

## Need For New Energy Sources



- *If we continue to burn fossil fuels for energy, they will only last another few hundred years.*

- This means that an energy shortfall could occur within the **next fifty years.**

# Nuclear Power



- Clean
- No CO<sub>2</sub>
- No immediate pollution problems with waste disposal
- Safety concerns

# Fusion Advantages

- Abundant fuel, available to all nations
  - Deuterium and lithium easily available for thousands of years
- Environmental Advantages
  - No carbon emissions, short-lived radioactivity
- Modest land usage
  - Compact relative to solar, wind and biomass
- Can't blow up
- Can produce electricity and hydrogen

# Fusion Disadvantages

- *Huge research and development costs*
- Radioactivity



Background

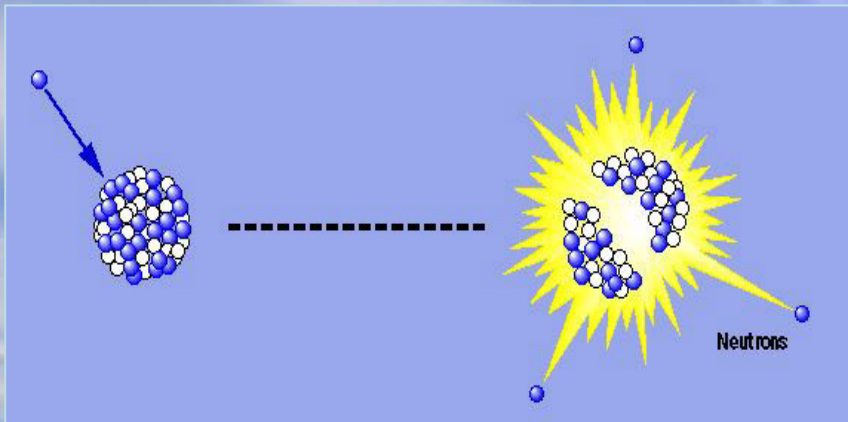
Fusion Basics



# Nuclear Power

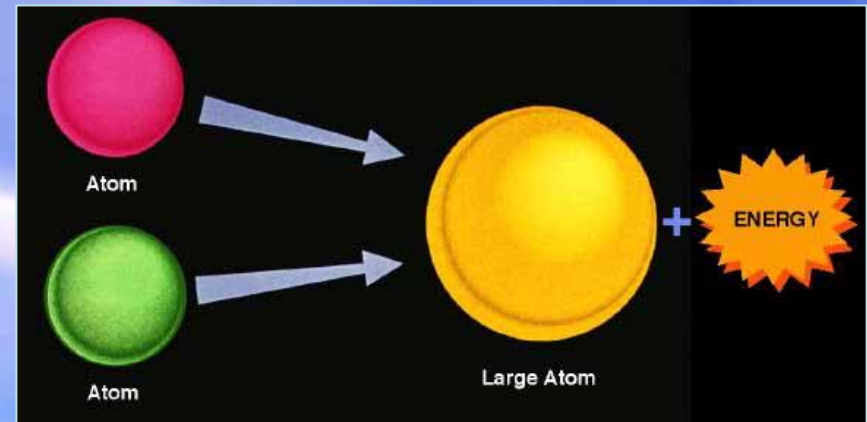
- Nuclear fission

- Where heavy atoms, such as uranium, are split apart releasing energy that holds the atom together

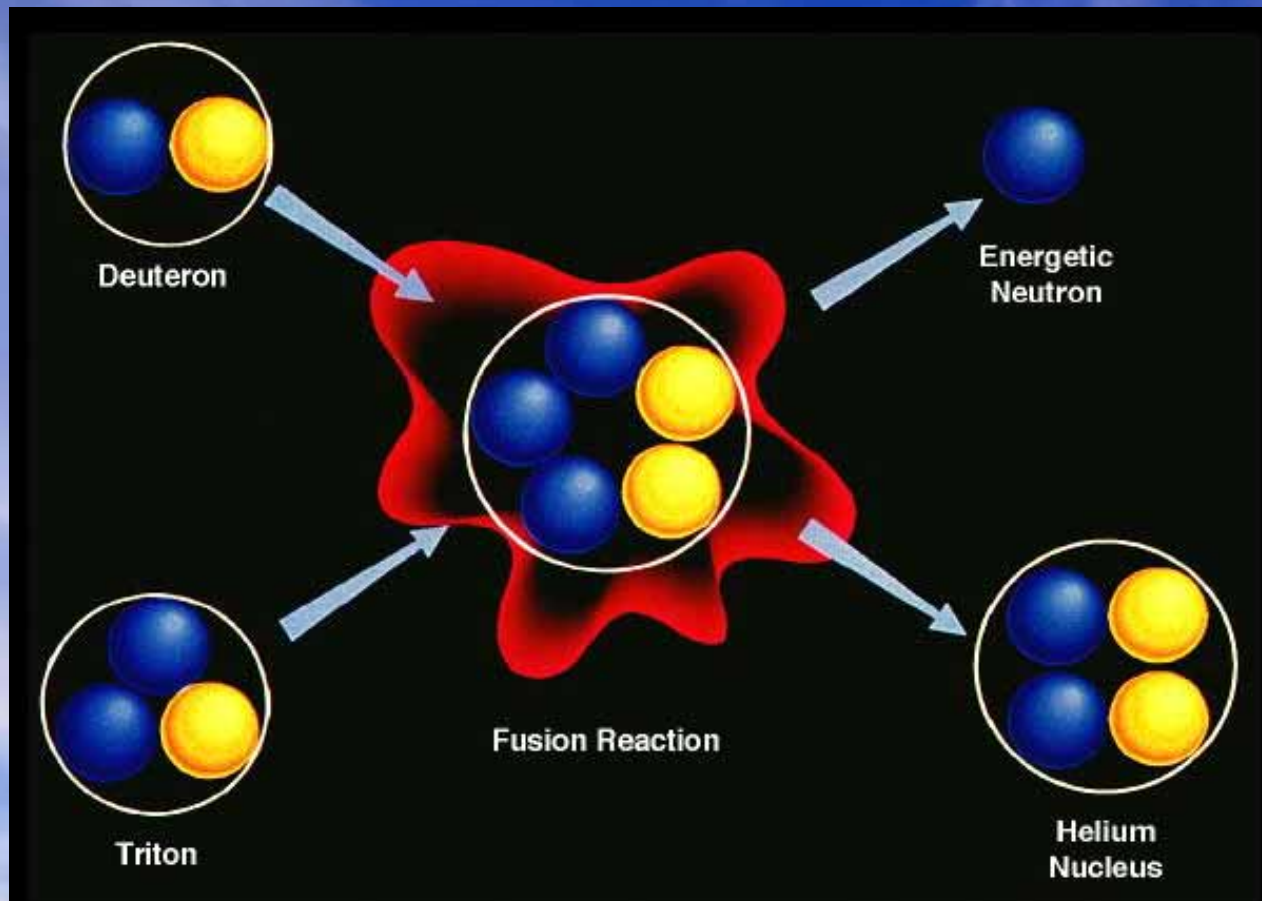


- Nuclear fusion



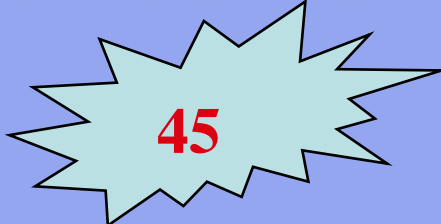
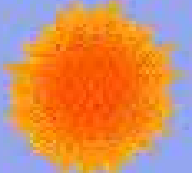


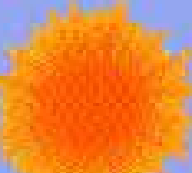

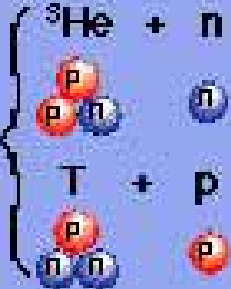


- Where light atoms, such as hydrogen, are joined together to release energy



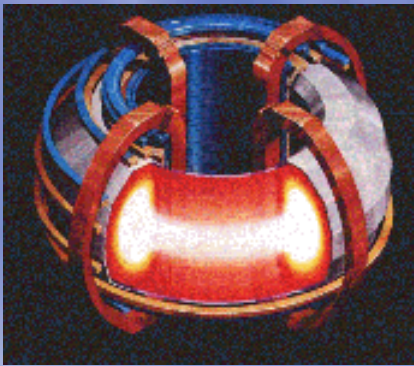
# Fusion Reaction with D-T



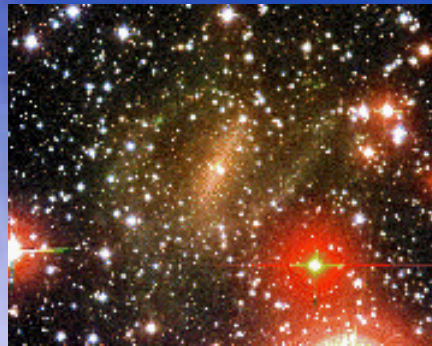
# Ideal Ignition Temperatures

Reaction		Ignition Temperature		Output Energy	
Fuel	Product	(millions of °C)	(keV)	(keV)	
$D + T$ 	${}^4\text{He} + n$ 	 45	4	 17,600	
$D + {}^3\text{He}$ 	${}^4\text{He} + p$ 		350	30	 18,300
$D + D$ 	$\left\{ \begin{array}{l} {}^3\text{He} + n \\ T + p \end{array} \right.$ 		400	35	 ~4,000
		400	35	 ~4,000	

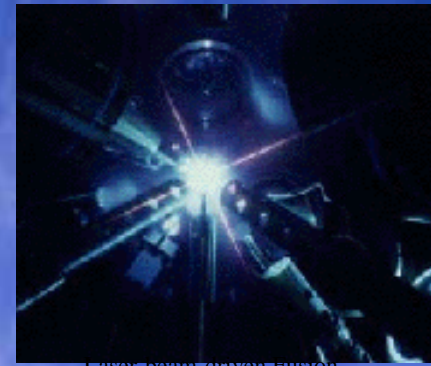
# Plasma Confinement & Heating



Tokamak Schematic



Stars & Galaxies



Laser-beam-driven Fusion

## Magnetic

- Electromagnetic Waves
- Ohmic Heating (by electric currents)
- Neutral Particle Beams (atomic hydrogen)
- Compression (by magnetic fields)
- Fusion Reactions (primarily D+T)

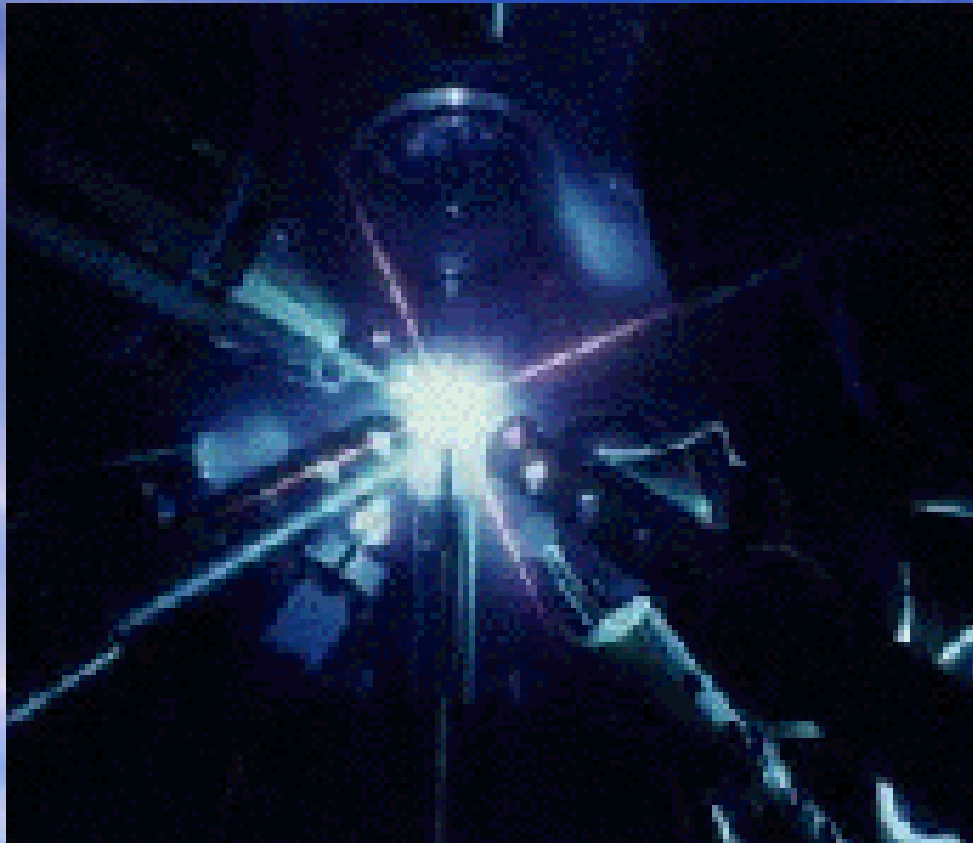
## Gravity

- Compression (gravity)
- Fusion Reactions (such as the p-p chain)

## Inertial

- Compression (implosion driven by laser or ion beams, or by X-rays from laser or ion beams)
- Fusion Reactions (primarily D+T)

# Inertial Confinement Fusion

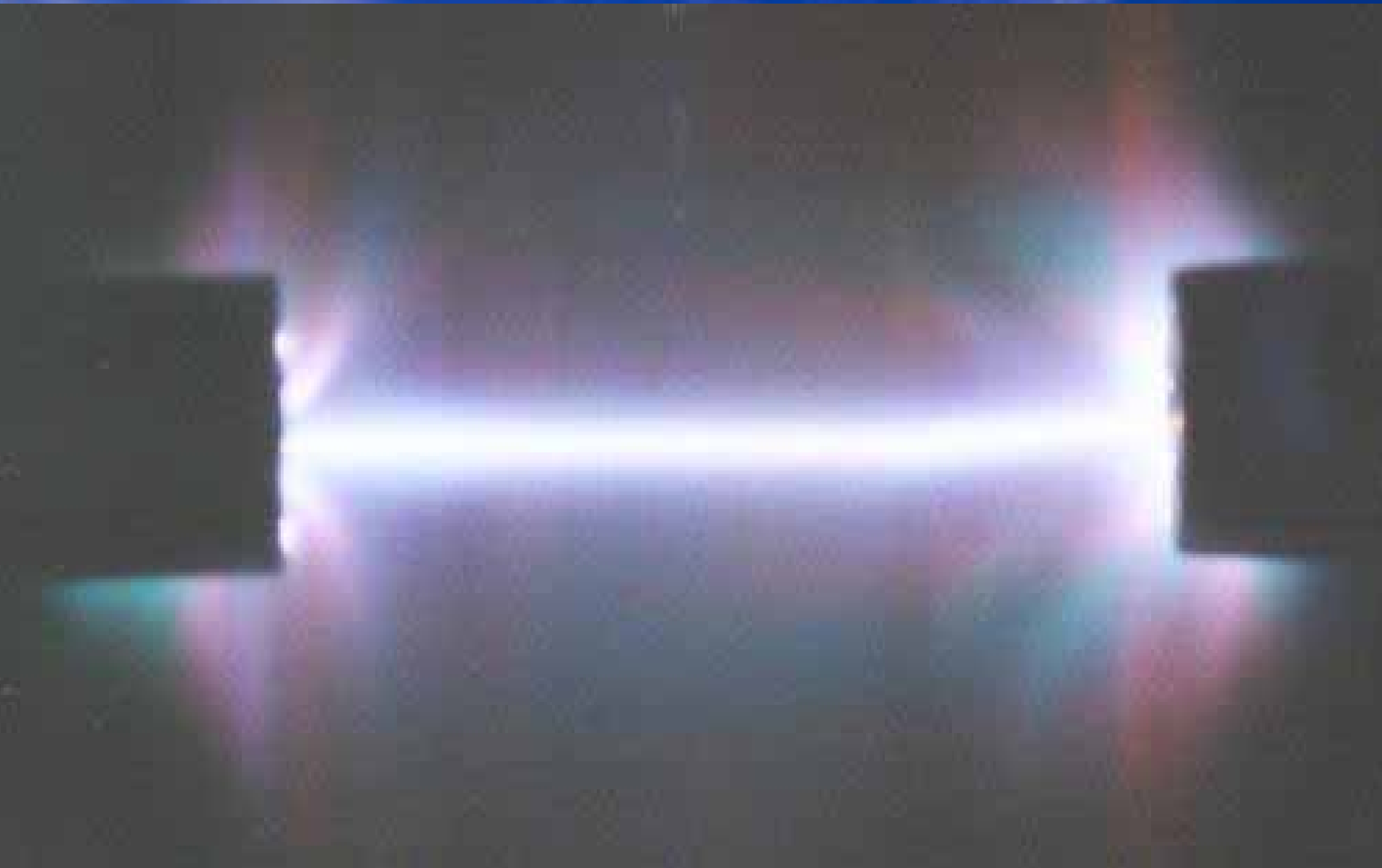


# Fusion By Magnetic Confinement

**Toroidal Magnetic  
Confinement of  
Plasma**



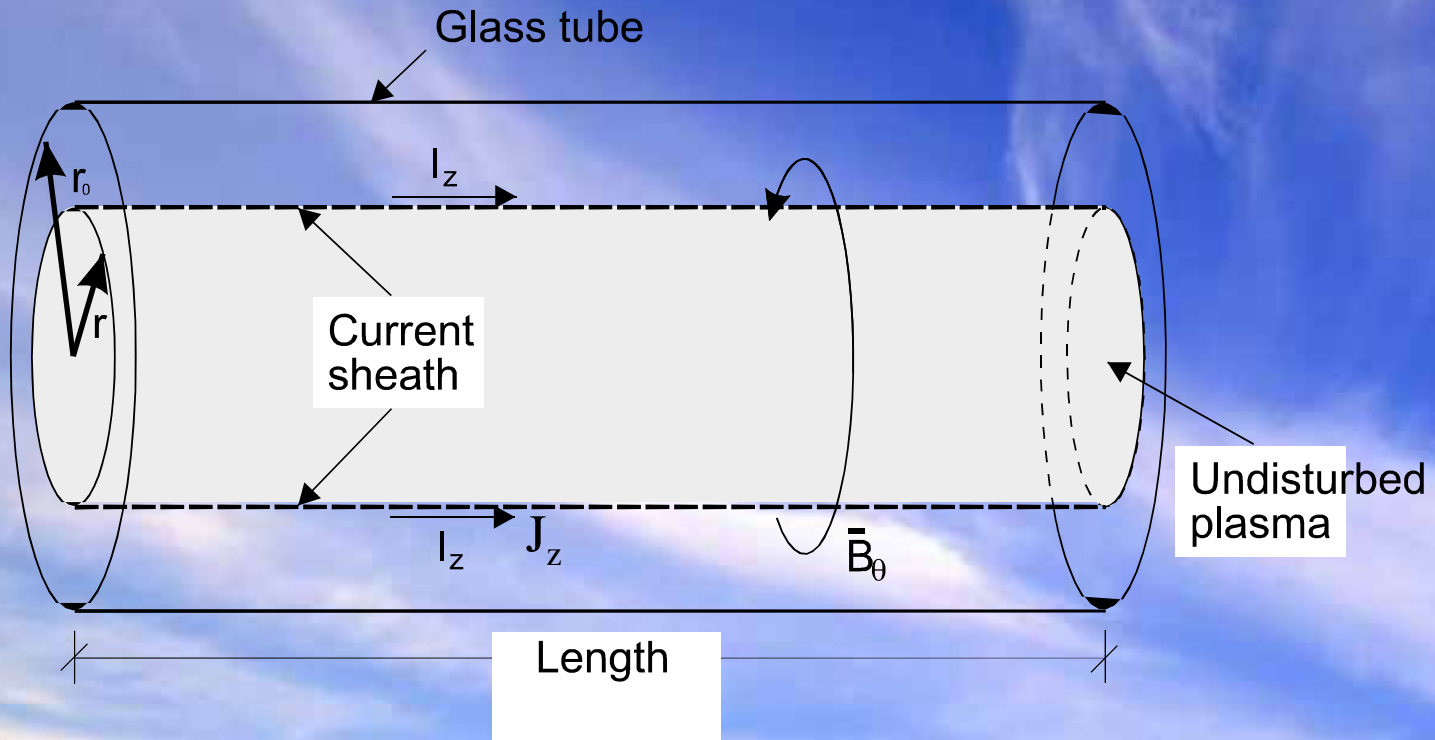
# Z-Pinch Device



# Introduction

## What is Z-pinch ?

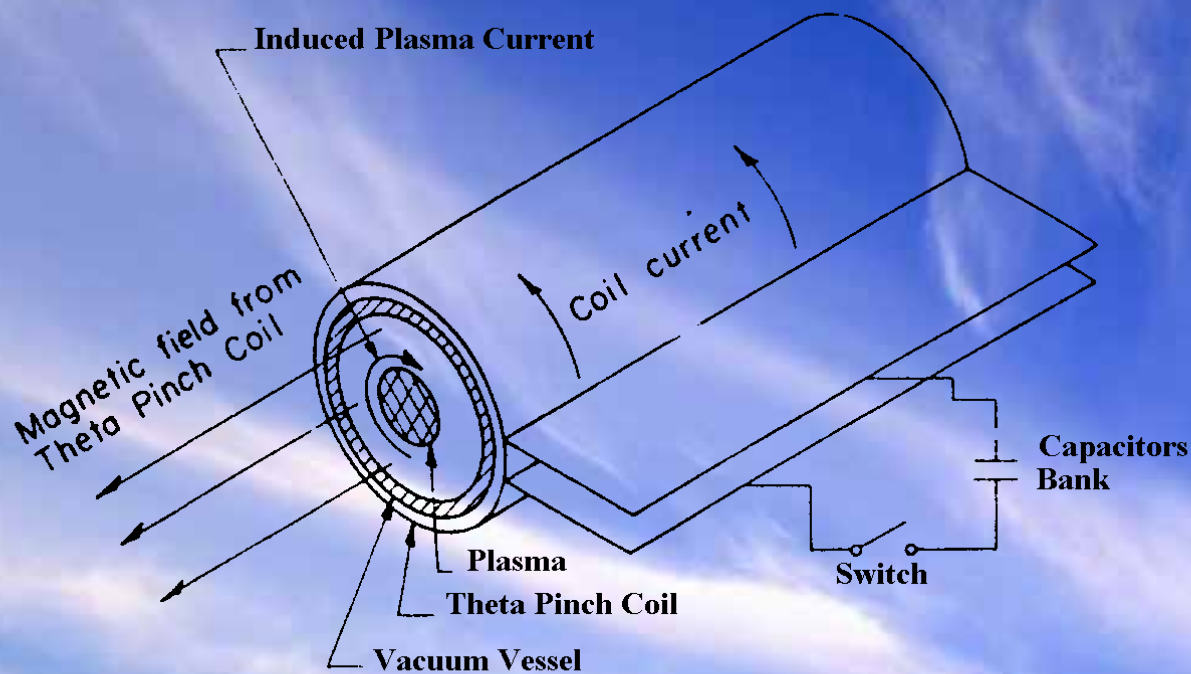
A plasma column in which current  $\mathbf{J}$  is driven in the axial ( $z$ ) direction by an electric power source producing an azimuthal ( $\theta$ ) direction magnetic field  $\mathbf{B}$  that tends to confine the plasma by a force ( $\mathbf{J} \times \mathbf{B}$ ).





# $\theta$ -pinch

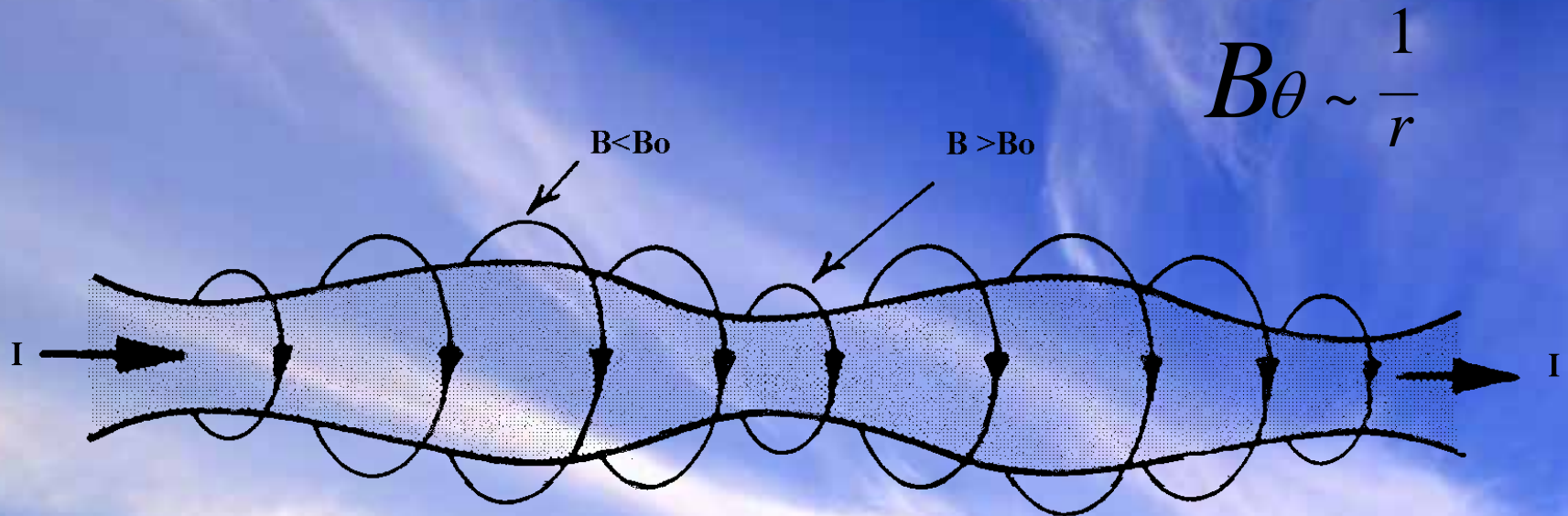
In  $\theta$ -pinch device the current flows in the azimuthal direction of cylindrical plasma column. The interaction of the current and axial magnetic field is through ( $\mathbf{J} \times \mathbf{B}$ ) force.



# Instabilities in Pinch Devices

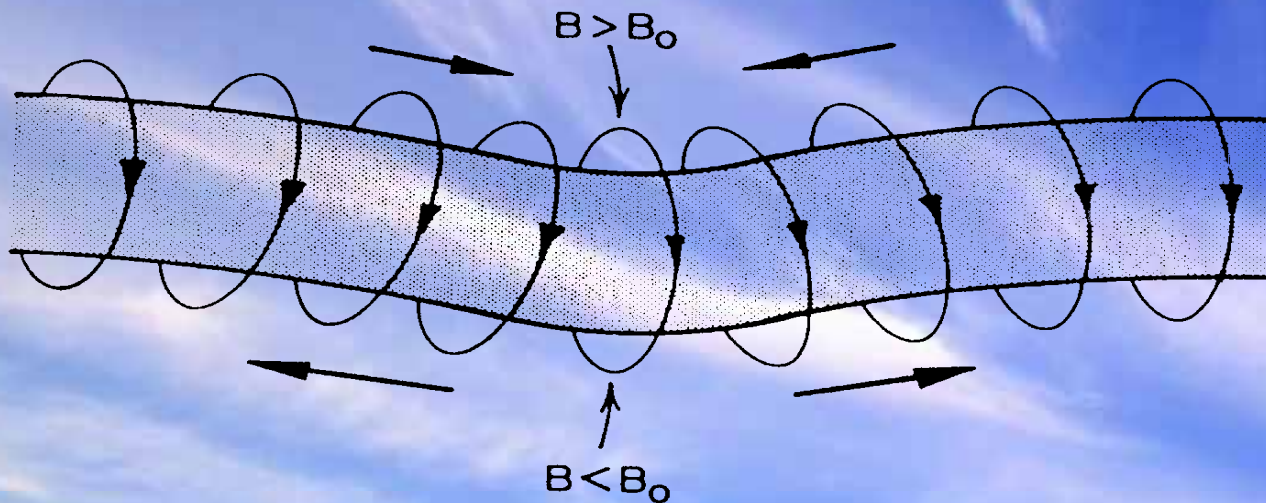
Plasma treated by MHD equations admits number of instabilities like **sausage**, **kink** and **Rayleigh-Taylor**.

## Sausage Instability



# Kink Instability

The kink instability arises due to the formation of bend or kink in the plasma column, although it maintains its uniform circular cross-section. *The density of the magnetic field lines increases on the concave side and decreases on the convex side.* The growth of the instability can be minimized by applying **axial magnetic field**.



# Rayleigh-Taylor Instability

Rayleigh-Taylor instability occurs when a **heavy fluid** is supported by **light fluid** in the presence of gravitational fields. In pinch devices **plasma being heavy fluid** is compressed by **massless magnetic field**. The instability occurs only if the plasma is **accelerating or decelerating**.



**The growth rate of R-T instability is given by**

$$\gamma = \sqrt{kg_{eff}}$$

$k$  is the wave number of the perturbation and  $g_{eff}$  is the acceleration of the plasma.

# Possible Ways to Mitigate R-T in Z-Pinches

R-T instability can be reduced with different stabilization techniques like.

- Spin of the outer shell,
- Thick shell
- Multi-gas-puff liner systems with the inclusion of axial magnetic field  $B_z$ .

# Major Applications of Z-pinches

- Controlled Thermonuclear Fusion
- Generation of High Magnetic Fields
- Sources of high energy, high intensity charged particles
- X-Ray Lasers etc.

# Numerical Model for Z-pinch dynamics

- **Snow plow model**

In this model we assume that

1. Plasma is good conductor; initially the discharge current form a **thin current sheath** on the surface of the plasma column.
2. Plasma ahead of the current sheath is in initial state.
3. The current sheath **sweeps all the mass in its way** as it moves.



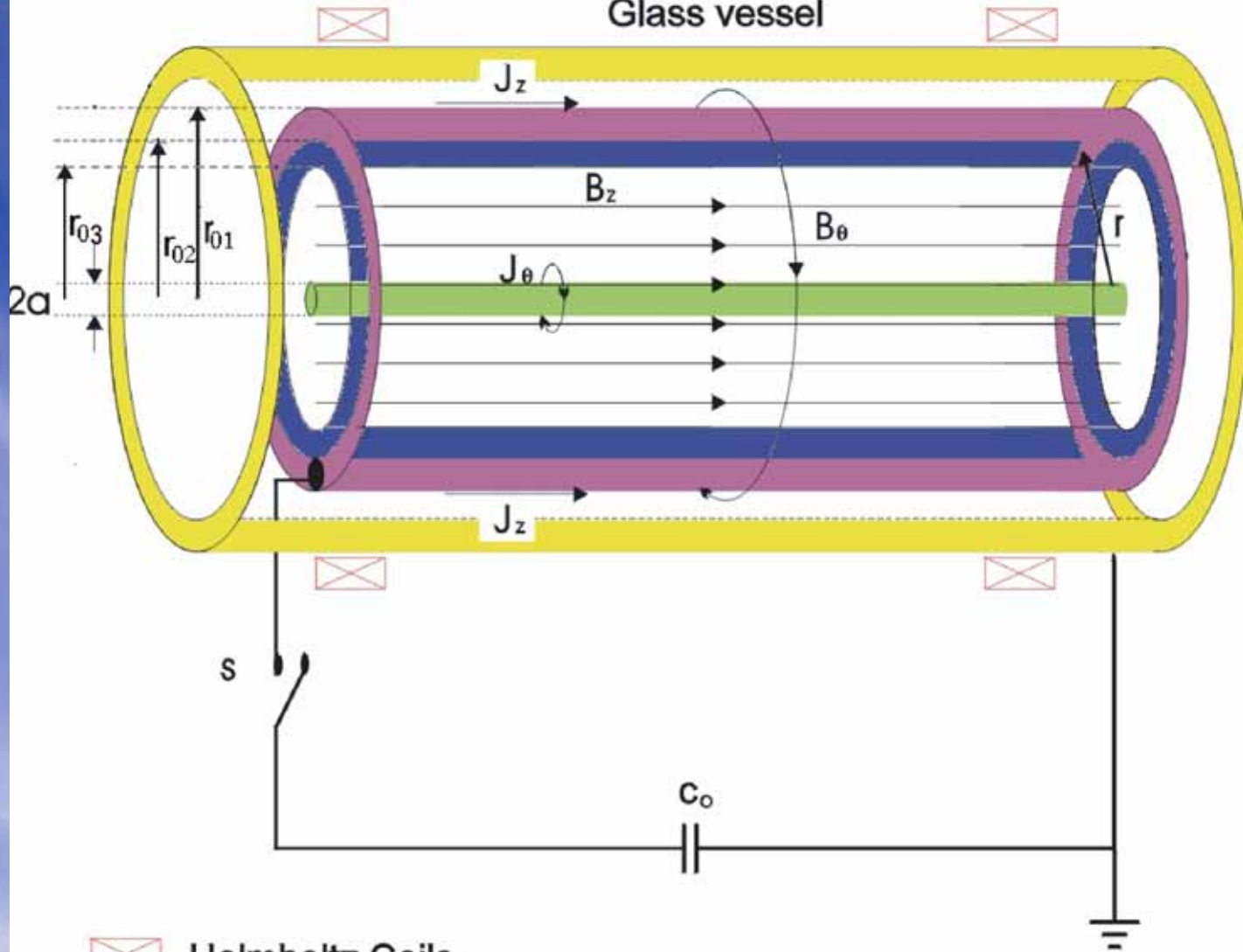
# Staged Pinch (Z- $\theta$ pinch)

The configuration embodies a conventional Z-pinch, imploding onto a co-axial cryogenic fiber ( $\theta$  -pinch) target plasma. This configuration is also called as Z-  $\theta$  pinch.

Addresses the problems of **effective compression** and **large current rising time**.

The inductive heating induces  $\theta$ -pinch discharge on the fiber surface with rise time of few nanosecond and the combined configuration of Z-  $\theta$  pinch is found stable.

Theoretical model for Z-  $\theta$  pinch have been proposed by *Rahman et al. (1989)*, assuming thin shell of the imploding Plasma.



⊞ Helmholtz Coils

■ Gas-Puff (I)

■ Gas-Puff (II)

■ D-T Fiber

## Two-Gas-Puff Liner System

# Dynamical Model of Staged Pinch

## • Outer Z-Pinch Dynamics

The dynamical equation for the outer double-gas-puff Z-pinch plasma based upon modified snow-plow model can be expressed as

$$\frac{d}{dt} \left( M \frac{dr}{dt} \right) = 2 \gamma \mathcal{P}_{mag} - P_{kin}$$

where  $M = 2 \gamma \mathcal{P}_0^2 r_1^2 = \mathcal{P}_1^2 r^2$  is the mass per unit length accumulated in the current sheath during the implosion.

The total magnetic pressure caused by azimuthal and axial magnetic fields can be written as

$$P_{mag} = \frac{1}{8 \gamma} \left[ \left( \frac{I_z}{5r} \right)^2 + B_0^2 \left( 1 - \frac{r_0}{r} \right)^4 \right]$$

Under adiabatic conditions, the kinetic pressure can be expressed as

$$P_{kin} = P_0 \left( \frac{r}{r_0} \right)^{\gamma}$$

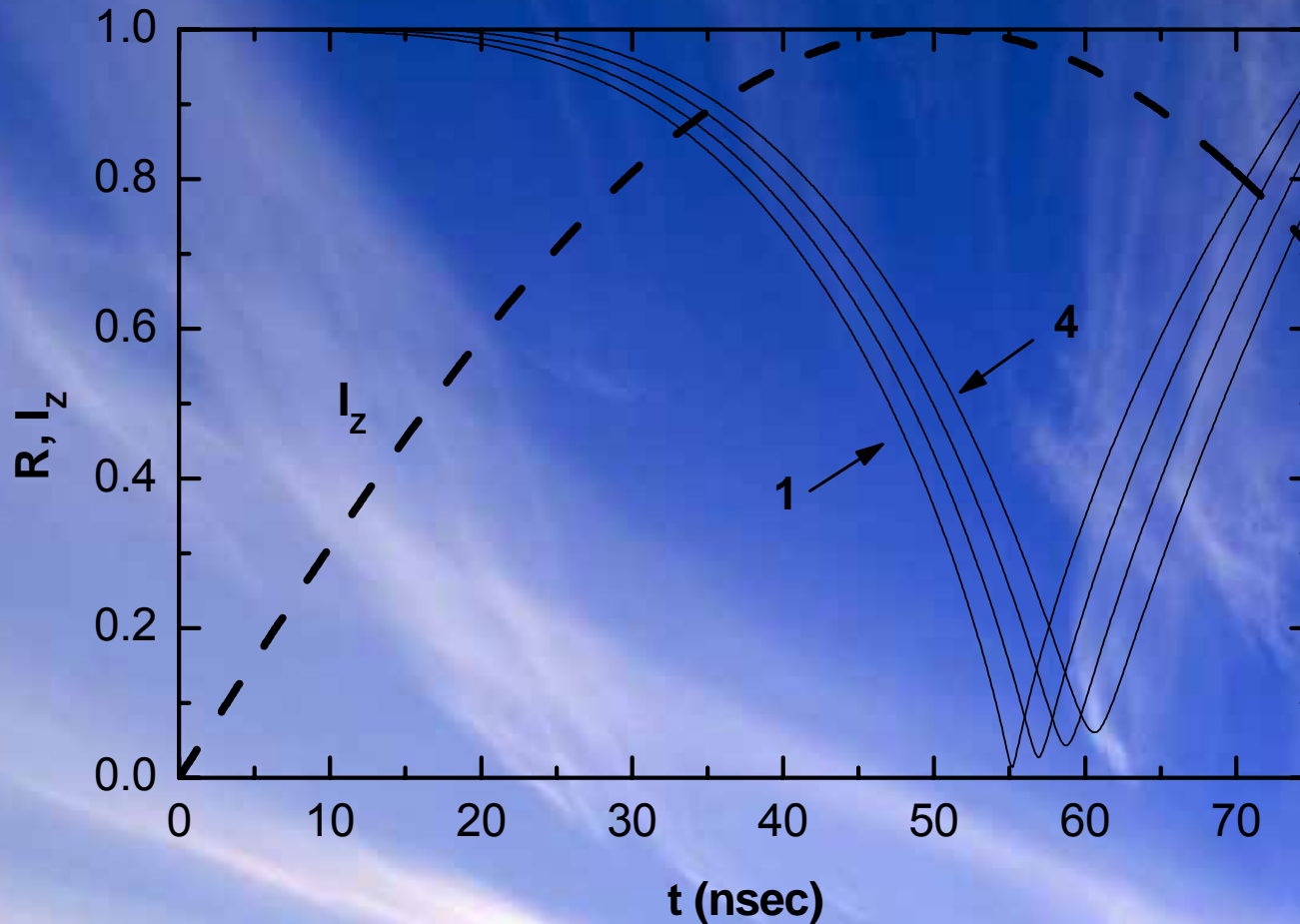
The equation of motion for the double gas puff Z-pinch plasma in the dimensionless form can be written as

$$\frac{d}{dt} \left[ \left( 1 - \beta R^2 \right) \frac{dR}{dt} \right] = \frac{a}{R} \left[ \sin^2 \left( \frac{\gamma}{2t_0} \right) - \frac{b}{R^2} \left( 1 - \beta R^2 \right) \right]$$

where  $R = (r/r_0)$  is the normalized radius,  $a = I_0^2 / 100 m_0 r_0^2$  is the measure of external force on the pinch per unit mass,  $b = (5 r_0 B_0^2 / I_0^2)^2$ ,  $\beta = 8 \pi P_0 / B_0^2$  and

$$\gamma = \frac{5}{2} \frac{I_0}{I_0} / \alpha \frac{I_0}{I_0} / r_0$$

*The above nonlinear differential equation is numerically integrated* for  $I_0 = 10$  MA,  $m_0 = 38 \mu$  g/cm,  $B_0 = 0.02$  MG,  $r_0 = 4$  cm and  $t_0 = 50$  nsec. Fig. 1 shows the evolution of the normalized outer z-pinch radius  $R$  and the normalized (by  $I_0$ ) current  $I_z$  versus time *for various values of  $\alpha$  and  $\beta$* . We see that the minimum radius of the imploding outer double gas-puff as a function of  $\alpha$  and  $\beta$ . For fixed value of  $\alpha$  ( $= 0.1$ ), finite  $\beta$ , always delays the maximum compression. **Small values of  $\beta < 0.1$  gives higher compression.** This indicates that double gas-puff devices can be used for controlled thermonuclear fusion. Whereas, for large  $\beta$  case, the maximum compression occurs at later times. Similarly, large  $\alpha$  with fixed  $\beta$  gives fast compression.



**Fig.1:** Normalized plots of axial current  $I_z$  and outer z-pinch radius  $R$  versus time, for different values of  $\beta$  and for  $\alpha = 0.1$ . Curves 1-4 for  $\beta = 0, 0.025, 0.050, 0.075$ , respectively.

# Dynamics of the Inner $\theta$ -pinch Fiber Plasma

Continuity equation

$$\frac{\partial n}{\partial t} + \nabla \cdot (nV) = 0$$

Mass conservation equation

$$mn \frac{dV}{dt} = P_{mag}$$

$$P_{kin} = (1 + Z)nT \quad P_{mag} = \frac{B_{\theta}^2}{8\pi} \left[ \frac{1}{R^4} + \left\{ 1 - \left( \frac{a_0}{a} \right)^4 \right\} \right]$$

Z being the charge state of the plasma ions.  $n$  is number density.

The energy equation under the adiabatic condition

$$n \frac{dT}{dt} = \frac{1}{2} \frac{d}{dt} \left( \frac{B_{\theta}^2}{4\pi} \right) - P_{ohm} - P_{alpha} - P_{loss}$$

Here, the Ohmic heating term in normalized parameters can be expressed as:

$$P_{ohm} = 1.29 \times 10^{21} \left( \frac{B_0^2}{a_0^2 T_0^{3/2}} \right) \frac{1}{a^2 T^{3/2} R^4}$$

The energy loss term includes the bremsstrahlung and the cyclotron radiation loss terms:

$$P_{brem} = 3.32 \times 10^{20} n_0^2 \left( \frac{\sigma T_0 \psi^2}{a^4} \right)$$

$$P_{cycl} = 3.88 \times 10^{16} \left( \frac{n_0 B_0^2 T T_0}{a^2 R^4} \right)$$

The alpha-particle self-heating term can be written as:

$$P_{alpha} = 3.22 \times 10^{26} \frac{n_0^2}{\sigma T_0 \psi^3} \left( \frac{1}{a^2} 2n_\alpha \right)^2 \exp\left( \frac{19.94}{\sigma T_0 \psi^3} \right)$$

where  $n_\alpha$  can be obtained from the production rate equation

$$\frac{dn_\alpha}{dt} = \frac{9.2n_0}{\sigma T_0 \psi^{3/2}} \left( \frac{1}{a^2} 2n_\alpha \right)^2 \exp\left( \frac{19.94}{\sigma T_0 \psi^3} \right) - \frac{2n_\alpha}{a} \frac{da}{dt}$$

Here  $P_{Ohm}$ ,  $P_{brem}$ ,  $P_{cycl}$  and  $P_{alpha}$  are in units of keV/(nsec-cm<sup>3</sup>);  $a_0$ ,  $B_0$  and  $T_0$  are in units of  $\mu$  m, MG, and keV, respectively.

The fiber plasma equations in the normalized form can be expressed as

$$\frac{d^2 a}{dt^2} + \frac{200 B_0^2}{n_0 a_0^2} \left[ \frac{a}{R^4} - 800 \left( \frac{n_0 T_0}{B_0^2} \right) \frac{T}{a} - a \left( 1 - \frac{1}{a^4} \right) \right]$$

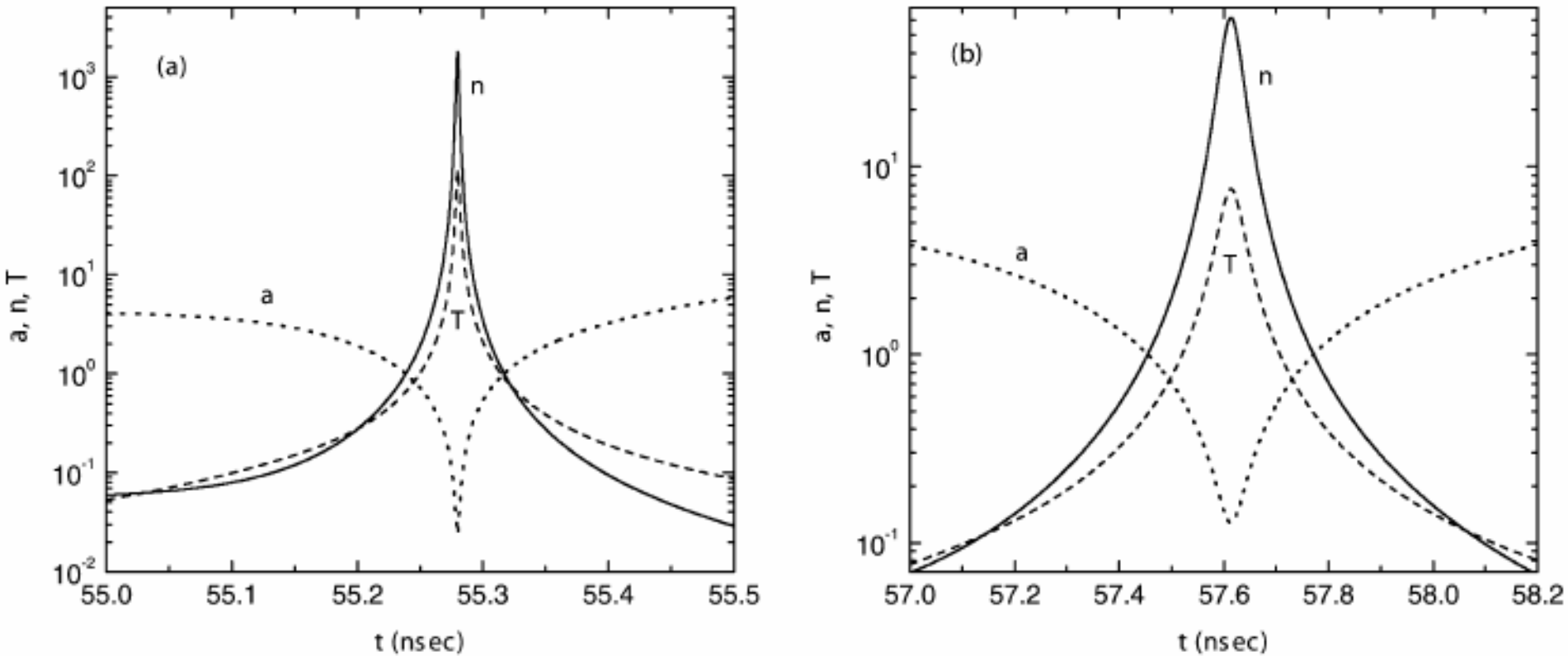
$$\frac{dT}{dt} + \frac{200 B_0^2}{n_0 a_0^2} \left[ \frac{a}{R^4} - 800 \left( \frac{n_0 T_0}{B_0^2} \right) \frac{T}{a} - a \left( 1 - \frac{1}{a^4} \right) \right] \frac{da}{dt} = \frac{10^{22} a^2}{2 T_0 n_0} \left( P_{ohm} + P_{alpha} - P_{brem} - P_{cycl} \right)$$

where the fiber radius  $a$  and the temperature  $T$  are normalized to their initial values  $a_0$  and  $T_0$ ,  $n_0$  being the initial density of the fiber plasma in the units of  $10^{22} \text{ cm}^{-3}$ .

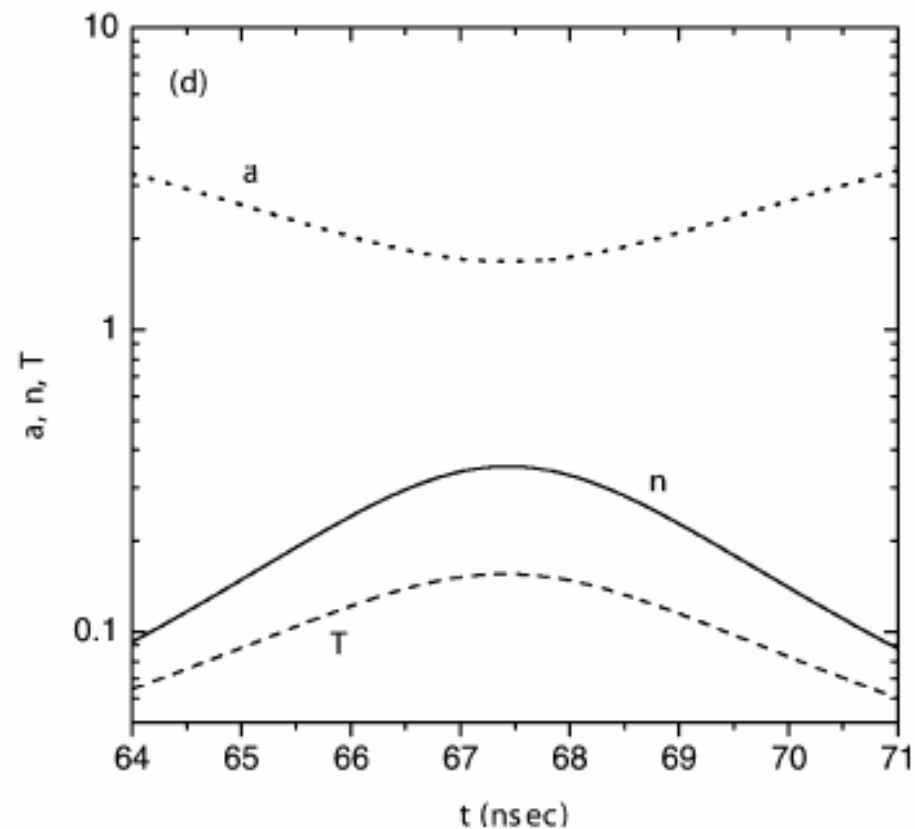
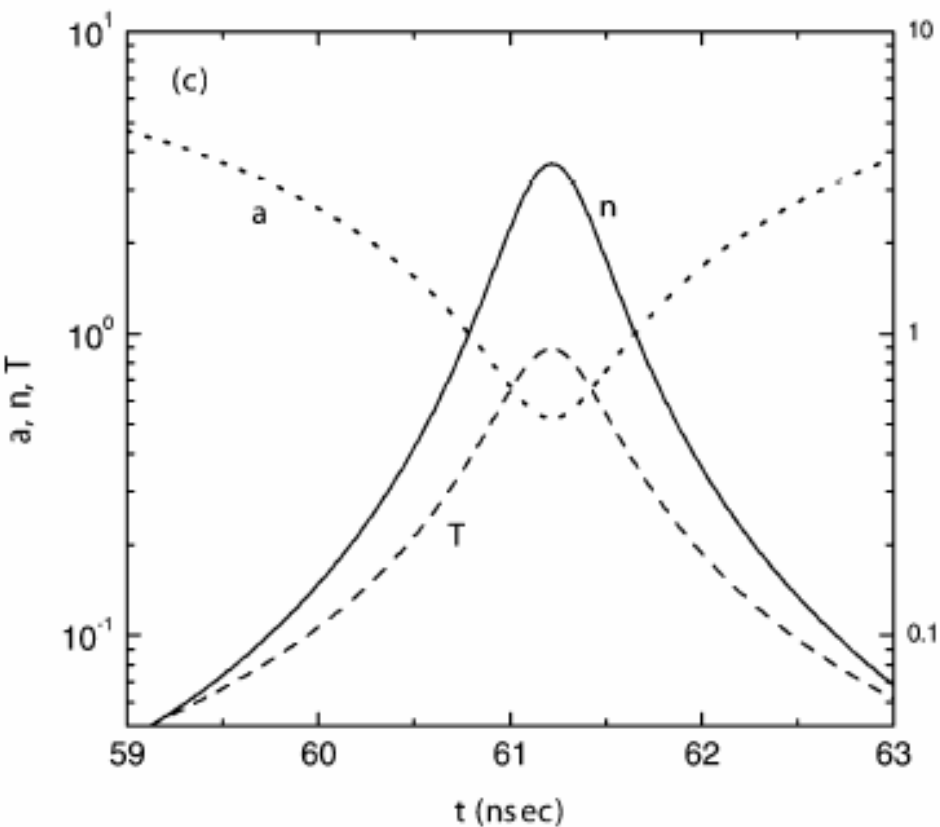
## Numerical Results and Discussion

Using the typical parameters of the University of California-Irvine experiments, we have numerically integrated the above equations with  $I_0 = 10 \text{ MA}$ ,  $r_{\square} = 4 \text{ cm}$ ,  $t_0 = 50 \text{ nsec}$ ,  $M_{01} = 38 \text{ } \mu\text{g/cm}$ ,  $T_0 = 20 \text{ eV}$ ,  $B_0 = 20 \text{ kG}$ ,  $a_0 = 0.02 \text{ cm}$ ,  $n_0 = 10^{22} \text{ cm}^{-3}$  for different values of  $\alpha$  and for  $\beta$  in the range  $0 \leq \beta \leq 0.075$ . Figure 2(a-d) displays the results for the normalized radius  $a$ , density  $n$  and temperature  $T$  as a function of time during the final stages of collapse for a D-T  $\theta$ -pinch plasma when ohmic heating, adiabatic heating,  $\alpha$ -particle self-heating and radiative losses are included for different values of  $\beta$  with  $\alpha = 0.1$ .

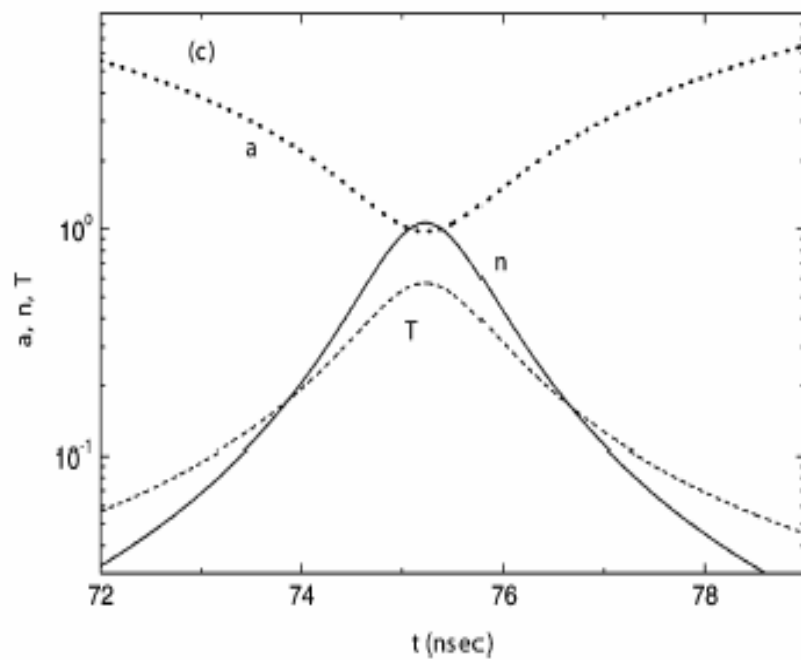
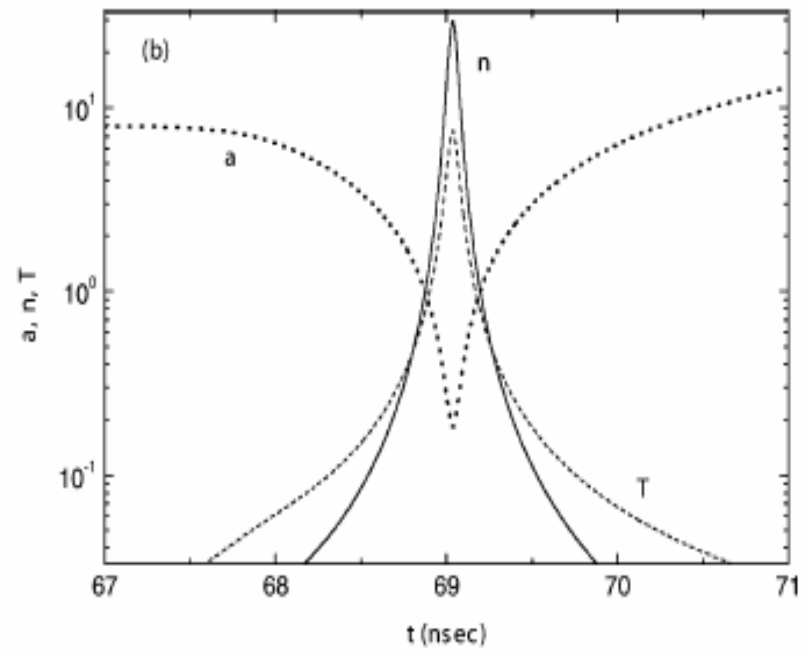
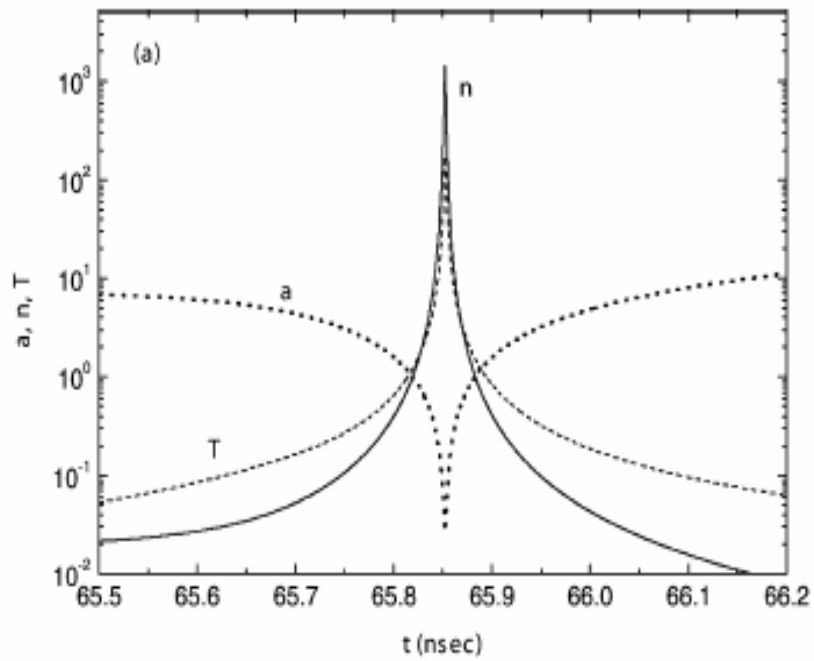




**Fig.2 (a, b):** Dynamics of the  $\theta$ -pinch displaying the plots of the normalized fiber radius  $a$ , normalized number density  $n$  ( $10^{22} \text{ cm}^{-3}$ ) and temperature  $T$  ( $\text{k eV}$ ) versus time during the last stages of compression with  $\alpha = 0.1$  and for different values of  $\beta$ . Curves 1-4 for  $\beta = 0, 0.025, 0.050, 0.075$ , respectively.



**Fig.2 (c, d):** Dynamics of the  $\theta$ -pinch displaying the plots of the normalized fiber radius  $a$ , normalized number density  $n$  ( $10^{22} \text{ cm}^{-3}$ ) and temperature  $T$  (k eV) versus time during the last stages of compression with  $\alpha = 0.1$  and for different values of  $\beta$ . Curves 1-4 for  $\beta = 0, 0.025, 0.050, 0.075$ , respectively.



For  $\alpha = 0.5$

It is evident from the graphs that without the kinetic pressure term ( $\beta=0$ ), one can obtain high density ( $n \sim 10^{25} \text{ cm}^{-3}$ ) and high temperature ( $T \sim 100 \text{ keV}$ ) plasma with  $\alpha = 0.1$ . However, for any finite- $\beta$  value with fixed  $\alpha = 0.1$ , seems to reduce the maximum compression, and leads to lower temperatures and densities.

For example, for  $\beta = 0.025$ , the maximum density (Fig. 2(b)) at peak compression is about  $100 n_0$  and the temperature is about  $10 \text{ keV}$ . On the other hand, for  $\beta = 0.075$ , the maximum density (Fig.2(d)) at peak compression is about  $0.3 n_0$  with a temperature of the order of  $0.05 \text{ keV}$ .

On the other hand, if we choose a relatively large value of  $\alpha = 0.5$ , then the maximum density and temperature at peak compression drastically reduces (see e.g., Fig. 3(a)-(c)) for any finite  $\beta$ .

**From these results one may conclude** that the double gas-puff staged pinch *can be used for controlled thermonuclear fusion with small  $\beta$  and high  $\alpha$  values*. Our numerical results demonstrates that **large  $\alpha$**  (for a large density ratio of the test to the driver gas at the interface position) **gives fast compression** while **high- $\beta$  gives slow compression**. The **finite- $\beta$  effect also delays the timing of the maximum compression**. Thus for optimum choice of  $\alpha$  and  $\beta$  parameters, the double gas-puff staged pinch can be used as a more feasible approach to achieve fusion conditions with enhanced stability.

# Questions



# Thanks !

## References:

- 1) Physica Scripta, vol. **72**, 399 - 403 (2005).
- 2) Modern Physics Letters B, vol. **19**, 1095 - 1105 (2005).